Embroidered Rectangular Split-Ring Resonators for the Characterization of Dielectric Materials

Shahrzad Zahertar, Emma Laurin, Linzi E. Dodd, and Hamdi Torun, *Member, IEEE*

***Abstract*— In this paper, we report an embroidered rectangular split-ring resonator (SRR) operating at S band for material characterization based on the differences in dielectric parameters. We designed, fabricated and characterized SRR sensors on a conventional fabric that can be conformally attached over the surface of samples under investigation. The structures are made of conductive threads and can be embroidered on any dielectric fabric at low cost using conventional embroidery methods. We have demonstrated material characterization capability of the sensors using a specific design with a length of 60 mm and a width of 30 mm. We wrapped the sensors on low-density polyethylene (LDPE) bottles filled with deionized (DI) water and common solvents (ethanol, methanol, isopropanol and acetone) in our experiments. We measured the nominal resonant frequency of a specific sensor wrapped around an empty bottle as 2.07 GHz. The shifts in resonant frequencies when the bottle was filled with the solvents follow the dielectric constants of the solvents.**

***Key Words*— split-ring resonator; metamaterials; embroidered sensors; microwave sensors**

I. Introduction

Split-Ring resonators (SRR) are the basic building blocks for metamaterials. SRR structures have been successfully demonstrated for the control and manipulation of electromagnetic waves in a broad spectral range from microwaves [1] to terahertz [2] and infrared [3]. The geometry of the structure, usually a circular or rectangular metallic ring with one or multiple splits, determines the frequency of operation. Structures with millimeter- to centimeter-scale are usually employed as microwave resonators. The structures are driven in electrical resonance when they polarize electric field or when they support induced circulating current over their surface. The resonance is known as an electric resonance in the former case, and a magnetic resonance in the latter case. Any change in the geometry or electrical characteristics of the medium alters the resonant frequency as the polarization of the electric field or induction of the circulating current relies on the effective capacitance and inductance defined by the structure. Tracking the changes in resonant frequency has been exploited as an effective sensing mechanism to determine changes in the geometry of SRR structures [4] and in the permittivity of the environment[5]–[10]. This is especially advantageous since the quality factor of the resonators can be over 1000 in microwave band [11].

Flexible sensors have been at the focus of delivering mechanically conformal structures for various applications including smart skins, wearable devices and microfluidic platforms. SRR structures fabricated on thin flexible substrates have been introduced as flexible devices. Among these, different configurations based on conventional metallic electrodes on flexible substrates such as polypropylene [12], polyimide [13] and poly-ethylene terephthalate(PET) [14] have been reported. Another configuration is based on inkjet-printed electrodes on PET [15]. The electrodes can also be defined using silver conductive paint as reported for strain sensing on a flexible latex substrate [4]. In an unconventional implementation, liquid metal (Galinstan) electrodes were employed in a microfluidic channel made of polydimethylsiloxane (PDMS) [16]. Also, a substrate-free configuration made of conductive rubber was reported for strain sensing applications [17].

An emerging field for the realization of flexible devices is embroidery that has been used to deliver electronic textiles using inherently flexible conductive threads on flexible fabric substrates. The developments in new electronic elements and interconnects in electronic textiles have made it possible to develop devices for a range of wearable applications from sensors to computers [18], [19]. Conductive threads, as the basic interconnect element that are inherently flexible has enabled the realization of metallic structures on conventional fabrics. Antennas are typical examples for which the whole structure can be implemented using only conductive threads[20]. Similar to antennas, metamaterials based on SRRs

An earlier version of this paper was presented at the 2019 IEEE International Conference on Flexible and Printable Sensors and Systems (FLEPS) and was published in its Proceedings; DOI: 10.1109/FLEPS.2019.8792233.

S. Zahertar is with Department of Mathematics, Physics and Electrical Engineering, Northumbria University, Newcastle upon Tyne, NE1 8ST, UK (e-mail: shahrzad.zahertar@northumbria.ac.uk).

Emma Laurin is with Université de Poitiers, IUT Mesures Physiques Chatellerault, 86100 Châtellerault, France (email: emma.laurin@etu.univ-poitiers.fr)

L.E. Dodd is with Department of Mathematics, Physics and Electrical Engineering, Northumbria University, Newcastle upon Tyne, NE1 8ST, UK (e-mail: linzi.dodd@northumbria.ac.uk).

H. Torun is with Department of Mathematics, Physics and Electrical Engineering, Northumbria University, Newcastle upon Tyne, NE1 8ST, UK (e-mail: hamdi.torun@northumbria.ac.uk).

[21]–[23] and radio frequency identification (RFID) tags [24] are usually realized using a few layers of metallic structures on fabrics for sensing and electromagnetic signal conditioning applications.

In this work, we report an embroidered rectangular SRR operating at S band for material characterization based on the differences in dielectric parameters. The SRR geometry is based on a previous work of ours, using which we investigated the operating principles of rectangular SRRs and explained an unexpected observation based on a particular excitation of the structures that induces magnetic resonance [25], [26]. The rectangular SRR configuration with the particular excitation method is advantageous for sensing applications. We fabricated a new structure using a conductive thread, which contains 316L stainless steel fibers on a calico cotton fabric. We employed this structure as a flexible sensor that can be wrapped around samples to measure their electromagnetic properties. The sensor is electrically passive and can be measured wirelessly. Our method can be used for the measurement of arbitrary geometries for material characterization applications attributed to the mechanically conformal structure and the wireless readout capability. The breadth of applications in material characterization using microwave-based sensors have been expanding including biosensing, impurity measurements, ensuring food safety and quality assessment [27]–[34].

II. Materials and Methods

We fabricated the SRR sensors using an embroidery machine (Brother PR1050X) with stainless-steel conductive threads (Sparkfun). A typical sensor and its dimensions are shown in Fig. 1. We fabricated the designs using a 6 mm wide design consisting of a 4 mm wide satin 'fill' stitch, an overlapping line stitch around the edge with a zig-zag width of 1.5 mm, both with a stitch density of 4.5 lines/mm and 7 rows of under sewing to reduce the resonator impedance. We measured the sheet resistance of the resonator as 4.67 m Ω-per-square. We implemented an inverted methodology to create the stitch patterns, whereby we placed the conductive thread in the lower bobbin of the embroidery machine, while we used standard polyester thread (#50, Brother) as the top spool thread. We used high thread tensions to reduce the amount of polyester thread visible on the conductive side of the design and to ensure the correct dimensions of the resonator design. Furthermore, we used the combined satin fill stitch and line edging pattern to ensure accuracy of the design width, as previous experiments using a wider satin stitch without an edge were generally too thin, compared to their design parameters, caused by this stitch pull-through effect. This approach ensured that the parameters of the fabricated resonator matched that of the design. We also used tear away stabilizer on the underside of the design to provide additional stability and to reduce fabric gather, which could have further affected the critical dimensions.

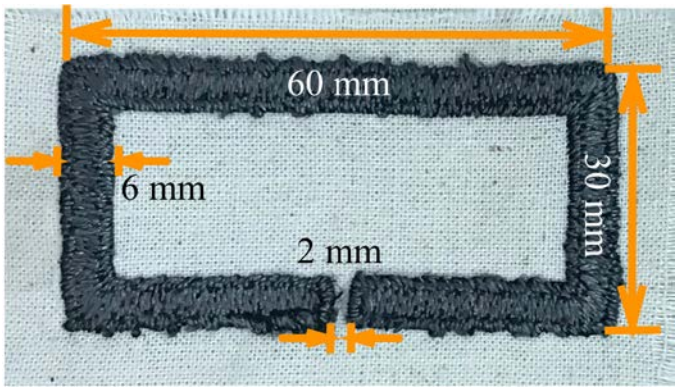

Fig. 1. Photograph of the fabricated SRR structure with a single split using an inverted embroidery method.

Then, we attached the embroidered sensor on curved surfaces of low-density polyethylene (LDPE) bottles for measurements using a vector network analyzer (VNA, Agilent N5230A PNA – L) as shown in Fig. 2. We used a pair of monopole patch antennas with a length of 30 mm and a width of 3.5 mm to excite the resonators while we measured s_{21} spectra between the ports of the VNA. During our measurements, we measured the spectra when the LDPE bottle was empty and filled with deionized water and different solvents of ethanol, methanol, and isopropanol (IPA) and acetone. We repeated the measurements for each case for 15 times.

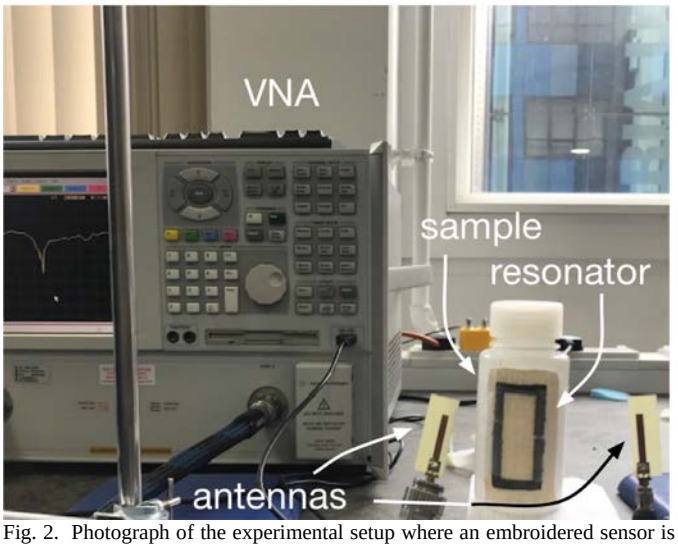

Fig. 2. Photograph of the experimental setup where an embroidered sensor is attached to an LDPE bottle filled with solvents.

We modelled the electromagnetic behavior of the resonators using commercially available electromagnetic simulation software (CST Studio Suite, Darmstadt Germany).
We used plane wave conditions for the excitation of the structures with different boundary conditions. We varied the relative permittivity of the medium in our simulations to model the presence of the fabric substrate and the LDPE bottle during the measurements. We used an effective relative permittivity value of 1.4 that matches well with the different modes of resonances we report in this paper.

III. Results and Discussion

Fig. 3 (a) shows the simulated s21 spectra for a specific excitation condition, where the electric field is along short sides of the SRR, the magnetic field is along long sides of the SRR, and the propagation vector is perpendicular to the surface of the resonator. When the electric field is along the short sides, the field can induce dipole formation along the direction of electric field. If the field is strong enough for the dipole formation and if the geometry of the structure can support this, two similar circulating current paths that are flowing in opposite directions are created as shown in Fig. 3 (b). We observe this formation indicating an electric-field assisted magnetic resonance at two distinct frequencies. When we aligned the antennas to support this excitation, we clearly observed the second resonance at 2.07 GHz. Our experimental results show the first resonance in this band to be broad and at 1.74 GHz. The experimental spectrum is presented after the values are normalized to the maximum value of s21 in the measurement band. The monopoles antennas have omnidirectional radiation pattern and can be used to excite different modes of resonances. Hence, it is also possible to excite a coupled mode, and the experimentally measured first resonance can be a result of a coupled mode. We varied the directions of field vectors to observe different modes of resonances using our simulation model.

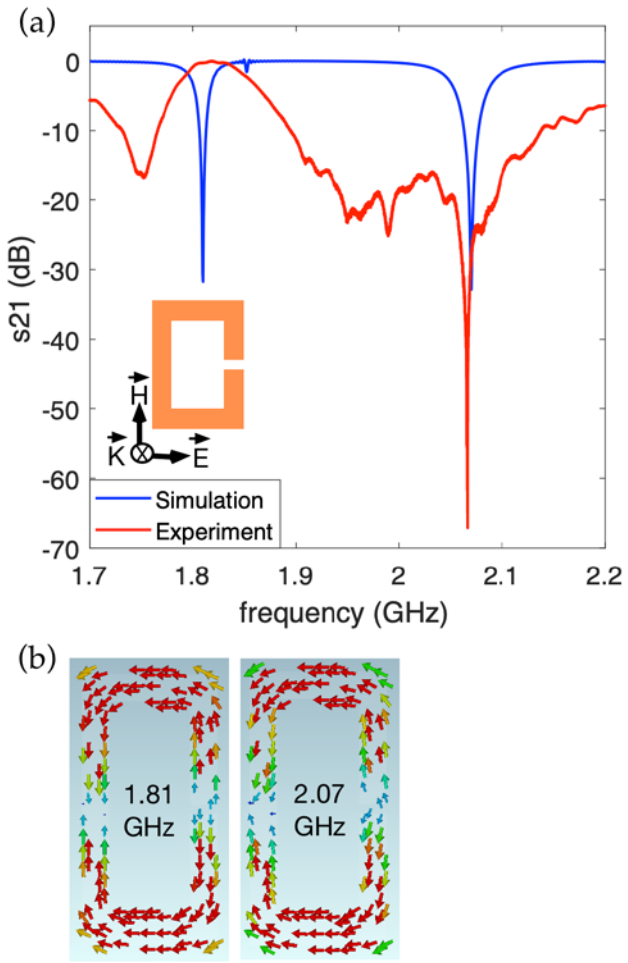

Fig. 3. (a) Simulation and experimental results (b) Current density patterns at 1.81, and 2.07 GHz for the excitation configuration shown in the figure.

Fig. 4 (a) shows the simulation results for another excitation condition, where the propagation vector is along short sides of the resonator, the electric field is along long sides of the resonator, and the magnetic field is perpendicular to the surface of the SRR. When the electric field is along the long side of the structure, it is possible to form an electrical dipole along this side rather than forming patterns of circulating current. Thus, this configuration excites electric resonances. Fig. 4 (b) shows the patterns of current densities at four different resonant frequencies in this band. The resonances within the simulation range indicates the incidences of electric field polarization. The efficient polarization occurs at 2.07 GHz where the incident power is dissipated effectively across the resonator as observed with a deeper signature of s21 spectrum. We also measured the spectrum after we aligned the antennas to excite these resonances. Fig. 4 (a) shows the experimentally obtained spectrum after the values are normalized to the maximum value of s_{21} in the measurement band. The additional resonance at 1.95 GHz observed in Fig. 4 (a) as compared to the results of Fig. 3 (a) indicates the excitation of the device supports the polarization of the electric field along the gap. This resonance corresponds to the resonance we observed at 1.93 GHz in our simulations.

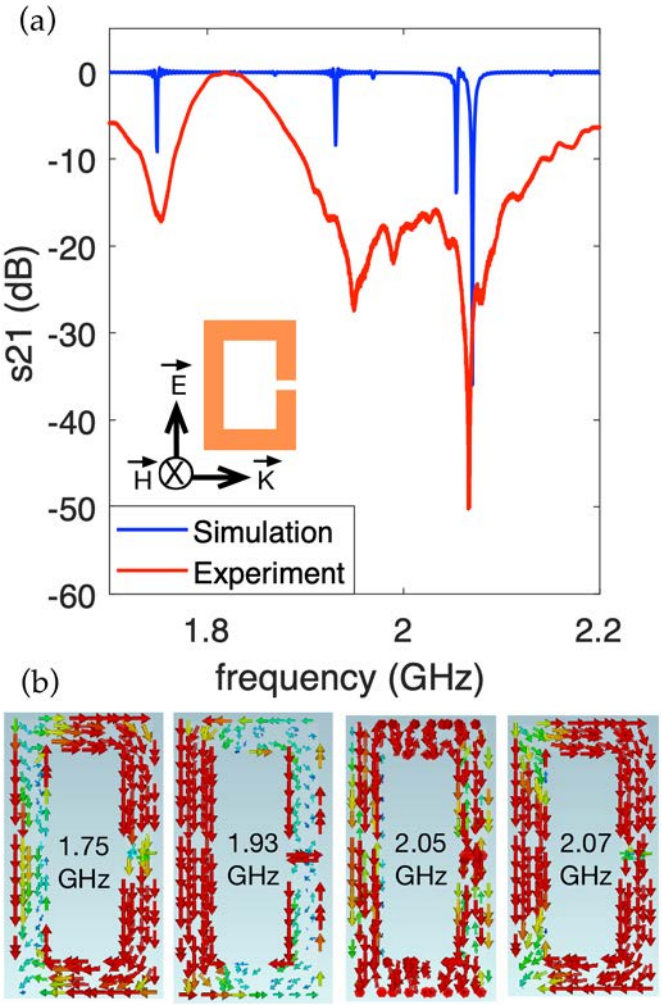

Fig. 4. (a) Simulation and experimental results (b) Current density patterns at 1.75, 1.93, 2.05, and 2.07 GHz for the excitation setting shown in the figure.

Experimentally obtained spectra shown in Fig. 3 (a) and Fig. 4 (a) show different resonant frequencies that can be used for sensing applications. The electromagnetic simulations help us to understand the nature of these resonances. Among these, the second resonance in Fig. 3 (a) at 2.07 GHz exhibits the highest quality factor with a value of 2070. In addition, it is the result of a magnetic resonance where the current path can be altered easily when the dielectric parameters of the medium are altered. Consequently, we monitored this resonance for sensing applications. The resonant frequency, f_0, is determined by the effective capacitance, C_{eff}, and the inductance, L_{eff}, of the device along the path of the circulating current as given in equation 1.

$$f_0 = \frac{1}{2\pi\sqrt{L_{eff}C_{eff}}} \quad (1)$$

The circulating current density for the second resonance in Fig. 3(b) at 2.07 GHz reveals two identical paths where the effective capacitance is determined by the nodal points, i.e. the gap and the mid-point along the long side of the rectangle to the left of the gap. The capacitance associated with the surface charges is known as surface capacitance and is contributing to the effective capacitance in addition to the gap capacitance [1]. Each capacitance term is proportional to the permittivity of the medium. Hence, the change in permittivity results in a change in resonant frequency. The structure can be optimized for permittivity sensing based on a specific resonant mode by ensuring the current is interacting with the environment.

We tracked the resonant frequency of the resonator when it was attached to LDPE bottles filled with DI water, methanol, ethanol, IPA, and acetone. Each solvent has a different relative permittivity, leading to a different value of effective capacitance along the current path shown in Fig. 3 (b). Thus, a change in relative permittivity results in a change in resonant frequency. The relative permittivity for DI water, methanol, ethanol, acetone, IPA, and air are 80, 32.6, 22.4, 20.6, 18.3, and 1 respectively [35].

Fig. 5(a) shows a set of experimentally obtained s21 spectra for different solvents and the empty bottle. Each spectrum is presented after it is normalized in the measurement band. The measured frequencies for DI water, methanol, ethanol, acetone, IPA, and empty bottles are 1.88, 1.89, 1.90, 2.01, 2.05, and 2.07 GHz, respectively. The values of quality factor at resonance are in the range of 2010 and 5265. The measured values of quality factor correspond to a frequency resolution of 1 MHz within the measurement range. This is a narrower range as compared to the spectra of Fig. 3, tracking the second frequency in that figure. The order of frequencies is in agreement with the values of relative permittivity for the samples. The dependency of the resonant frequency to the value of relative permittivity is shown in Fig. 5(b). We measured samples with relative permittivity values distributed in a wide range within which we do not observe linear response. This is expected based on the operation of the sensor. The relative permittivity of the samples determines part of the effective capacitance term of equation 1 as the effective capacitance comprises the capacitance terms of the fabric, the bottle and the sample inside the bottle. The shifts in resonant frequencies indicate the changes in real part of the permittivity. The imaginary value of the permittivity contributes to the loss of the resonator and affects the quality factor at resonance. The quality factor of the resonator is determined by all the loss mechanisms in the system including the radiation loss of the resonator and the antennas together with the losses in the fabric, bottle and the sample. We have not observed significant and repeatable changes in quality factor of the resonator during our measurements.

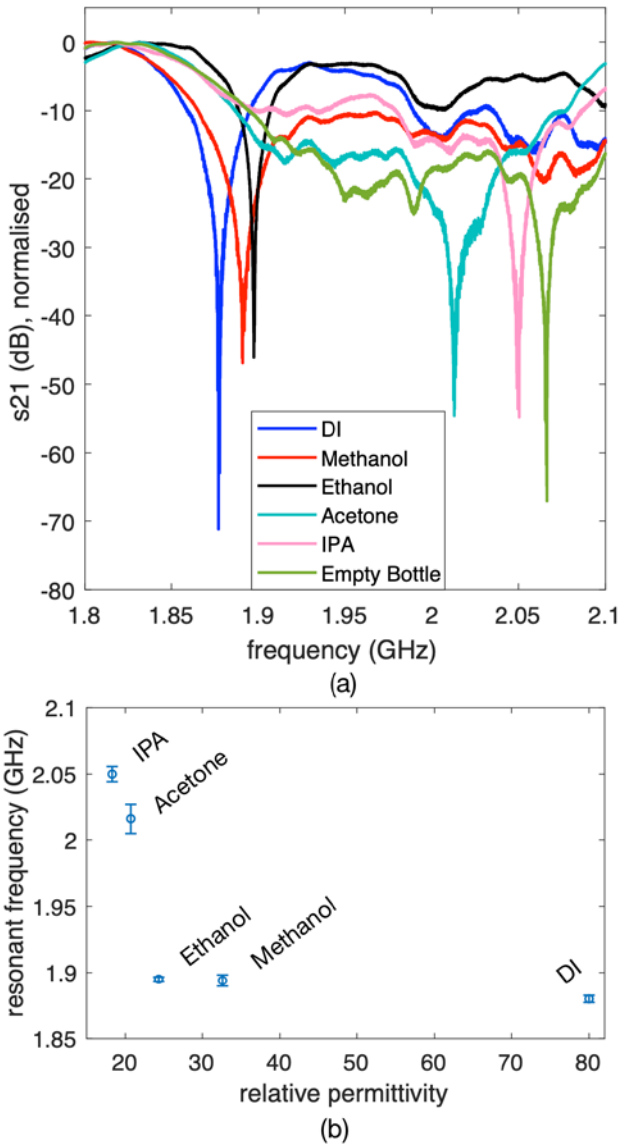

Fig. 5. (a) Normalized s21 spectra of the SRR structure, where the sensor is wrapped around the LDPE bottles filled with DI water, methanol, ethanol, acetone, IPA, and empty bottle. (b) Measured resonant frequencies for different bottles.

We repeated the measurement for 15 times to assess the repeatability. Fig. 6 depicts the histograms of the measured frequencies for the solvents and the empty bottle. Table 1 summarizes the material properties and the mean values of measured frequencies.

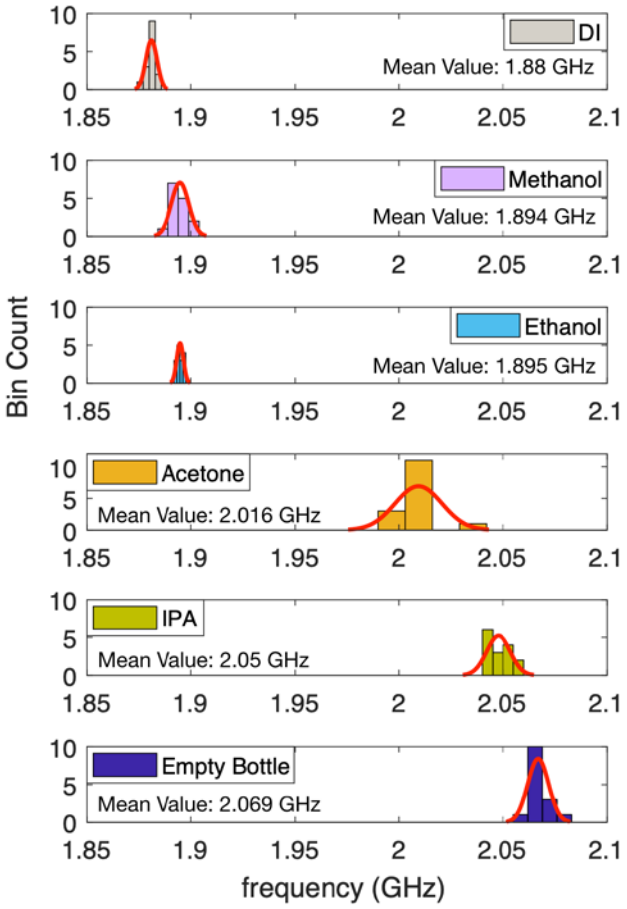

Fig. 6. Histogram and mean value of the set of experiments for solvents and empty bottle.

TABLE I
MATERIAL PROPERTIES AND THE MEAN VALUE OF THE MEASURED FREQUENCIES FOR SOLVENTS.

Material	Relative Permittivity	Resonant Frequency (Mean ± Standard Deviation) (GHz)
Deionised Water	80	1.88 ± 0.0027
Methanol	32.6	1.894 ± 0.0042
Ethanol	24.3	1.895 ± 0.0016
Acetone	20.7	2.016 ± 0.0112
Isopropanol	18.3	2.05 ± 0.0057
Air	1	2.069 ± 0.0050

IV. CONCLUSION

In this paper, we introduce an embroidered rectangular SRR for material characterization applications. We fabricated SRR using a conductive thread by implementing embroidery methods on an ordinary fabric substrate. The architecture is advantageous for the applications where the sensor needs to be conformally covering sample surfaces. As a case study, we wrapped the SRR around LDPE bottles filled with DI water and different solvents. We experimentally demonstrated that the solvents can be identified by tracking the resonant frequency of

the SRR, exploiting the fact that the changes in relative permittivity of the samples result in changes in resonant frequency. Also, we investigated different modes of resonances with the help of electromagnetic simulations. We identified the modes to select the optimum one for sensing applications.

The embroidery method is advantageous for the fabrication of SRR-based sensors where the active device can be defined using a single layer of metallization. This method can be applied to define SRR-based sensors, filters and absorbers on flexible substrates and daily items such as cloth. Our study is focused on a device that can be used as a method for substance characterization and has a potential in identifying impurities in liquids for contamination measurements. This configuration can be extended to wearable sensing scenarios where the sensors can be implemented on a conformal structure that can be wrapped around arbitrary shapes depending on the needs. The fabrication method is simple, cost-effective and allows the realization of the sensors very quickly. We plan to exploit this method to further develop sensors that can be used for harsh environment sensing especially with wearables attributed to the wireless sensing capability.

REFERENCES

[1] H. Torun, F. Cagri Top, G. Dundar, and A. D. Yalcinkaya, “An antenna-coupled split-ring resonator for biosensing,” J. Appl. Phys., vol. 116, no. 12, 2014.

[2] H.-T. Chen, W. J. Padilla, J. M. O. Zide, A. C. Gossard, A. J. Taylor, and R. D. Averitt, “Active terahertz metamaterial devices,” Nature, vol. 444, no. 7119, pp. 597–600, 2006.

[3] C. Rockstuhl et al., “Resonances of split-ring resonator metamaterials in the near infrared,” Appl. Phys. B Lasers Opt., vol. 84, no. 1–2, pp. 219–227, 2006.

[4] G. Ekinci, A. Calikoglu, S. N. Solak, A. D. Yalcinkaya, G. Dundar, and H. Torun, “Split-ring resonator-based sensors on flexible substrates for glaucoma monitoring,” Sensors Actuators, A Phys., vol. 268, pp. 32–37, 2017.

[5] A. Salim, S. Ghosh, and S. Lim, “Low-cost and lightweight 3D-printed split-ring resonator for chemical sensing applications,” Sensors (Switzerland), vol. 18, no. 9, 2018.

[6] E. Reyes-Vera, G. Acevedo-Osorio, M. Arias-Correa, and D. E. Senior, “A Submersible Printed Sensor Based on a Monopole-Coupled Split Ring Resonator for Permittivity Characterization,” Sensors (Basel)., 2019.

[7] W. Withayachumnankul, K. Jaruwongrungsee, A. Tuantranont, C. Fumeaux, and D. Abbott, “Metamaterial-based microfluidic sensor for dielectric characterization,” Sensors Actuators, A Phys., vol. 189, pp. 233–237, 2013.

[8] A. A. Abduljabar, D. J. Rowe, A. Porch, and D. A. Barrow, “Novel microwave microfluidic sensor using a microstrip split-ring resonator,” IEEE Trans. Microw. Theory Tech., vol. 62, no. 3, pp. 679–688, 2014.

[9] I. M. Rusni, A. Ismail, A. R. H. Alhawari, M. N. Hamidon, and N. A. Yusof, “An aligned-gap and centered-gap rectangular multiple split ring resonator for dielectric sensing applications,” Sensors (Switzerland), 2014.

[10] C. Sen Lee and C. L. Yang, “Complementary split-ring resonators for measuring dielectric constants and loss tangents,” IEEE Microw. Wirel. Components Lett., 2014.

[11] H. Torun, S. Sadeghzadeh, and A. D. Yalcinkaya, “Note: Tunable overlapping half-ring resonator,” Rev. Sci. Instrum., 2013.

[12] P. M. Ragi, K. S. Umadevi, P. Nees, J. Jose, M. V. Keerthy, and V. P. Joseph, “Flexible split-ring resonator metamaterial structure at microwave frequencies,” Microw. Opt. Technol. Lett., vol. 54, no. 6, pp. 1415–1416, Jun. 2012.

[13] R. Melik, E. Unal, N. Kosku Perkgoz, C. Puttlitz, and H. V. Demir, “Flexible metamaterials for wireless strain sensing,” Appl. Phys. Lett., vol. 95, no. 18, pp. 2–5, 2009.

[14] M. E. Jalil, M. K. A. Rahim, N. A. Samsuri, and R. Dewan, “Flexible printed chipless RFID tag using metamaterial–split ring resonator,” Appl. Phys. A Mater. Sci. Process., 2016.

[15] H. K. Kim, K. Ling, K. Kim, and S. Lim, “Flexible inkjet-printed metamaterial absorber for coating a cylindrical object,” Opt. Express, 2015.

[16] R. A. Awang, T. Baum, M. Nasabi, S. Sriram, and W. S. T. Rowe, “Mechanically tolerant fluidic split ring resonators,” Smart Mater. Struct., vol. 25, no. 7, 2016.

[17] F. Zhang, Z. Liu, K. Qiu, W. Zhang, C. Wu, and S. Feng, “Conductive rubber based flexible metamaterial,” Appl. Phys. Lett., vol. 106, no. 6, pp. 2–6, 2015.

[18] M. Stoppa and A. Chiolerio, “Wearable electronics and smart textiles: A critical review,” Sensors (Switzerland). 2014.

[19] K. Mondal, “Recent Advances in Soft E-Textiles,” Inventions , vol. 3, no. 2. 2018.

[20] J. Zhong, A. Kiourti, T. Sebastian, Y. Bayram, and J. L. Volakis, “Conformal Load-Bearing Spiral Antenna on Conductive Textile Threads,” IEEE Antennas Wirel. Propag. Lett., 2017.

[21] B. Moradi, R. Fernández-García, and I. Gil, “E-textile embroidered metamaterial transmission line for signal propagation control,” Materials (Basel)., 2018.

[22] M. S. Hesarian, S. S. Najar, and R. S. Shirazi, “Design and fabrication of a fabric for electromagnetic filtering application (Experimental and modeling analysis),” J. Text. Inst., 2018.

[23] F. Raval, S. Purohit, and Y. P. Kosta, “Dual-band wearable antenna using split ring resonator,” Waves in Random and Complex Media, vol. 26, no. 2, pp. 235–242, Apr. 2016.

[24] M. Hasani, A. Vena, L. Sydanheimo, L. Ukkonen, and M. M. Tentzeris, “Implementation of a dual-interrogation-mode embroidered RFID-Enabled strain sensor,” IEEE Antennas Wirel. Propag. Lett., 2013.

[25] S. Zahertar, A. D. Yalcinkaya, and H. Torun, “Rectangular split-ring resonators with single-split and two-splits under different excitations at microwave frequencies,” AIP Adv., 2015.

[26] S. Zahertar, L. E. Dodd, and H. Torun, “Embroidered Rectangular Split-Ring Resonators for Material Characterisation,” 2019.

[27] X. Zhang, C. Ruan, T. Ul Haq, and K. Chen, “High-sensitivity microwave sensor for liquid characterization using a complementary circular spiral resonator,” Sensors (Switzerland), vol. 19, no. 4, 2019.

[28] R. Joffe, E. O. Kamenetskii, and R. Shavit, “Novel microwave near-field sensors for material characterization, biology, and nanotechnology,” J. Appl. Phys., vol. 113, no. 6, 2013.

[29] K. Staszek, I. Piekarz, J. Sorocki, S. Koryciak, K. Wincza, and S. Gruszczynsk, “Low-cost microwave vector system for liquid properties monitoring,” IEEE Trans. Ind. Electron., vol. 65, no. 2, pp. 1665–1674, 2017.

[30] S. Ryynänen, “The electromagnetic properties of food materials: A review of the basic principles,” J. Food Eng., vol. 26, no. 4, pp. 409–429, 1995.

[31] O. Korostynska, R. Blakey, A. Mason, and A. Al-Shamma’A, “Novel method for vegetable oil type verification based on real-time microwave sensing,” Sensors Actuators, A Phys., vol. 202, pp. 211–216, 2013.

[32] S. Trabelsi and S. O. Nelson, “Microwave sensing of quality attributes of agricultural and food products,” IEEE Instrum. Meas. Mag., vol. 19, no. 1, pp. 36–41, 2016.

[33] M. H. Zarifi, M. Rahimi, M. Daneshmand, and T. Thundat, “Microwave ring resonator-based non-contact interface sensor for oil sands applications,” Sensors Actuators, B Chem., vol. 224, pp. 632–639, 2015.

[34] S. Trabelsi, A. W. Kraszewski, and S. O. Nelson, “A microwave method for on-line determination of bulk density and moisture content of particulate materials,” IEEE Trans. Instrum. Meas., vol. 47, no. 1, pp. 127–132, 1998.

[35] I. M. Smallwood, Handbook of organic solvent properties. Elsevier, 2004.

Shahrzad Zahertar is a PhD student at department of Mathematics, Physics and Electrical Engineering at Northumbria University, UK. She received her MSc degree in electrical and electronics engineering from Bogazici University, Turkey and BSc degree in electrical engineering-bioelectric from University of Tehran, Iran. Her current research interests include metamaterials for biosensing applications, Surface Acoustic Wave (SAW) biosensors, and Lab on Chip devices.

Emma Laurin received a scientific degree from the Institut Universitaire Technologique at Châtellerault named DUT Mesures Physiques. For this training she did an internship at Northumbria University where she was working on metamaterials. Currently, she's studying electrical engineering at the Conservatoire National des Arts et Metiers in Poitiers.

Linzi E. Dodd specializes in microsystems technology, fluid drag reduction, energy recovery and embroidered electronics. She joined Northumbria University in 2017, after 12 years at Durham University.

Hamdi Torun (HT) is a Vice-Chancellor's Senior Fellow at Northumbria University. Previously, he was an associate professor at Bogazici University, Turkey. He is a co-founder of GlakoLens, a biomedical spinoff company. He received Technology Award from Elginkan Foundation, Turkey in 2016, Young Scientist Award from The Science Academy, Turkey in 2016, Innovator Under 35 Award from MIT Tech Review in 2014, and Marie Curie Fellowship (MC-IRG Grant) in 2011. His expertise is in development of integrated micro/nanosystems especially for sensing applications.